Journal of Solid State Chemistry **151,** 330–334 (2000)
doi:10.1006/jssc.2000.8722, available online at http://www.idealibrary.com on IDEAL®

RAPID COMMUNICATION

Ru-Induced Ferromagnetism and Metallicity in Mn(IV)-Rich Manganites $Ln_{0.4}Ca_{0.6}MnO_3$

B. Raveau, A. Maignan, C. Martin, R. Mahendiran, and M. Hervieu

Laboratoire CRISMAT, ISMRA, 6 Boulevard du Maréchal Juin, 14050 Caen Cedex, France

Received February 4, 2000; in revised form March 7, 2000; accepted March 16, 2000

The doping of Mn sublattice by Ru in the Mn(IV)-rich manganites $Ln_{0.4}Ca_{0.6}MnO_3$ (*Ln*: Lanthanide; *Ln* = La, Pr, Nd, Sm) induces an insulator-to-metal transition which is not obtained by Cr doping. The appearance of metallicity and ferromagnetism in these Ru-doped manganites is explained in the frame of the phase separation scenario, Ru forming ferromagnetic (FM) clusters, which extend as the Ru content increases. The particular aptitude of Ru for promoting a FM metallic state is discussed, on the basis of Ru(V) and Ru(IV) oxidation states, which are isoelectronic to Mn(IV) and Mn(III), respectively. Magnetoresistance is also evidenced and discussed. © 2000 Academic Press

The important role of the mechanism of double exchange (DE) between Mn^{4+} and Mn^{3+} species in the magneto-transport properties of manganites with the perovskite structure (1–2) enables the colossal magnetoresistance (CMR) in those oxides to be either enhanced or induced by doping the Mn sites with adequate cations. In a great number of manganites, involving a transition from a ferromagnetic metallic to a paramagnetic activated state, it was shown that the substitution of various cations, such as Fe, Al, Sn, Ti, Mg, and Ga, for Mn decreases T_C but generally increases the CMR effect considerably (see Ref. (3) for a review). The most spectacular effect concerns the doping of the charge-ordered (CO) insulating manganites $Ln_{0.5}Ca_{0.5}MnO_3$ with Cr, Co, or Ni, which shows that an insulator-to-metal transition can be induced even in the absence of a magnetic field (4–6). In a recent study of the Cr-doped manganite $Nd_{0.5}Ca_{0.5}MnO_3$, Tokura and co-workers (7) showed that the fraction of the ferromagnetic phase embedded in the antiferromagnetic charge-ordered matrix can be controlled by the Cr content and by the magnetic field annealing and proposed that this doped manganite can be viewed as a relaxor ferromagnet. Coexistence of ferromagnetic metallic and paramagnetic insulating phases with charge-ordered regions was also proved using electron diffraction, and the possible decoupling of charge and orbital ordering was suggested in the Cr-doped $Pr_{0.5}Ca_{0.5}MnO_3$ manganites (8).

The possibility of inducing an insulator-to-metal (I–M) transition in the electron-rich manganites is not obvious. No I–M transition was observed as a result of Co or Ni doping, and only a reentrant I–M transition was obtained by Cr doping in the manganite $Pr_{0.4}Ca_{0.6}MnO_3$ (9). The recent results obtained by Rao and co-workers from the substitution of ruthenium for manganese in $Nd_{0.5}Ca_{0.5}MnO_3$ show that ruthenium is a new potential candidate since it induces I–M transition in this phase, T_C increasing with the Ru content (10). We believe that ruthenium, due to its two possible valencies Ru(V) and Ru(IV), with d^3 and d^4 electronic configurations, similar to Mn(IV) and Mn(III), respectively, should favor the DE in those materials. For this reason we have investigated the Ru doping of the Mn(IV)-rich manganites $Ln_{0.4}Ca_{0.6}MnO_3$. In the present paper, we show that an I–M transition in the absence of magnetic field can be induced in the CO $Ln_{0.4}Ca_{0.6}MnO_3$ oxides for the first time by Ru doping. Moreover, charge ordering tends to disappear rapidly for low Ru contents, and ferromagnetism is considerably increased up to 3 μ_B per Mn site, T_C increasing significantly with the Ru level.

The $Ln_{0.4}Ca_{0.6}Mn_{1-x}Ru_xO_3$ samples were synthesized using classical solid state reaction techniques by mixing the oxides Ln_2O_3 (*Ln* = La, Nd, Sm) or Pr_6O_{11}, CaO, MnO_2, and RuO_2 in stoichiometric ratios. The mixtures were then pressed into bars, heated to 1500°C in air for 12 h, and finally slowly cooled to 800°C and quenched to room temperature. The systematic investigation of the samples, using X-ray and electron diffraction, shows that they are single-phased, with an orthorhombic $GdFeO_3$-type structure. The room temperature X-ray patterns have been refined in the *Pnma* space group. The refined lattice volume and the orthorhombic distortion increase with the Ru content. For instance, in the samarium series, the cell parameters evolve

0022-4596/00 $35.00

from 5.3851(2) Å, 7.5280(3) Å, 5.3451(2) Å ($V = 216.68$ Å^3) for $x = 0$ to 5.4094(3) Å, 7.5546(4) Å, 5.3537(3) Å ($V = 218.78$ Å^3) for $x = 0.10$.

We focus first on the $La_{0.4}Ca_{0.6}Mn_{1-x}Ru_xO_3$ series. The resistivity curves $\rho(T)$ for these Ru-doped manganites in the absence of a magnetic field are shown in Fig. 1. Starting from the undoped compound ($x = 0$), which exhibits insulating behavior below $T_{CO} = 260$ K (inset of Fig. 1), the doping with Ru lowers the resistivity at low temperature in a spectacular way, i.e., by several orders of magnitude, leading to a "double bump" curve as shown for the $x = 0.04$ sample (Fig. 1, curve a). Note that this effect appears suddenly, since for $x = 0.02$ (not shown), the $\rho(T)$ curve is still similar to the curve for undoped manganite. For higher doping levels the resistivity is not significantly modified, as shown for the $x = 0.10$ sample (Fig. 1, curve b), where $\rho(T)$ is also characterized by two bumps. One remarkable feature of these resistivity curves is that the temperature of the first resistivity maximum, centered around 125 K, does not vary significantly with the doping level, whereas the temperature of the second maximum increases with the doping level from 240 K for $x = 0.04$ (Fig. 1, curve a) to 270 K for $x = 0.10$ (Fig. 1, curve b). The corresponding magnetization measured under 1.45 T versus temperature (Fig. 2) shows that the abrupt decrease in resistivity at low temperature is concomitant with the appearance of ferromagnetism (FM): for low doping levels ($x = 0.02$) the compound is antiferromagnetic; then the magnetic moment increases rapidly with x, and reaches a maximum value of 2.8 μ_B per Mn site at 4 K for $x = 0.06$, under 1.45 T. This rather high value of the magnetic moment clearly shows that FM is induced at a low temperature by Ru doping; moreover it can be seen that the Curie temperature, taken as the inflection point on the $M(T)$ curve, corresponds to the second resistivity maximum (Fig. 1). Thus, the Ru doping of $La_{0.4}Ca_{0.6}MnO_3$ tends to weaken the charge ordering and to induce ferromagnetism and metallicity at low temperature.

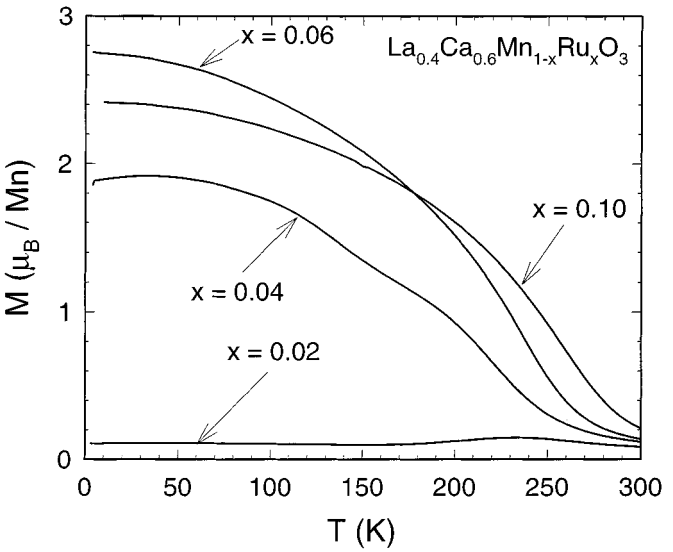

FIG. 2. T dependence of the magnetization (M) for $La_{0.4}Ca_{0.6}Mn_{1-x}Ru_xO_3$ (1.45 T, zero field cooling process). x values are labeled on the graph.

This particular effect of Ru doping can be generalized to other lanthanides. This is illustrated by the $\rho(T)$ and $M(T)$ curves of the Pr, Nd, and Sm manganites (Figs. 3–5). The $\rho(T)$ curves of the $x = 0.06$ and $x = 0.10$ samples of $Pr_{0.4}Ca_{0.6}Mn_{1-x}Ru_xO_3$ series (Fig. 3) show metallic behavior at low temperature, in contrast to the undoped phase which is

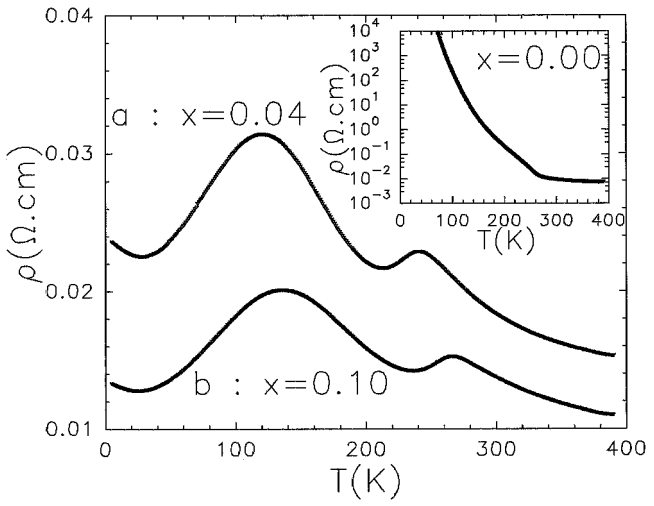

FIG. 1. T dependence of the resistivity (ρ) for $La_{0.4}Ca_{0.6}Mn_{1-x}Ru_xO_3$. Inset: $\rho(T)$ curve of the $x = 0.00$ sample.

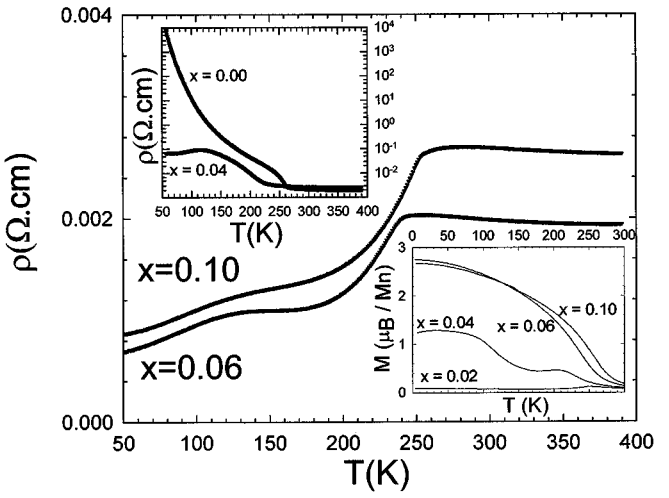

FIG. 3. $\rho(T)$ curves of $Pr_{0.4}Ca_{0.6}Mn_{1-x}Ru_xO_3$. Upper inset: $x = 0.00$ and $x = 0.04$ $\rho(T)$ curves. Lower inset: $M(T)$ curves of $Pr_{0.4}Ca_{0.6}Mn_{1-x}Ru_xO_3$.

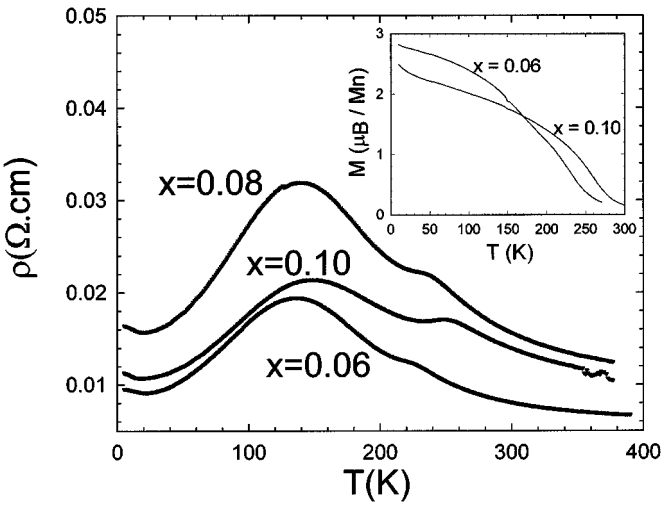

FIG. 4. $\rho(T)$ curves of $Nd_{0.4}Ca_{0.6}Mn_{1-x}Ru_xO_3$. Inset: $M(T)$ curves of $Nd_{0.4}Ca_{0.6}Mn_{1-x}Ru_xO_3$.

charge-ordered and consequently insulating below $T_{CO} =$ 260 K (upper inset of Fig. 3). As in the La manganites, we notice that FM increases with the Ru-doping level, reaching a magnetic moment of 2.8 μ_B and a T_C of 240 K for $x = 0.06$ (lower inset of Fig. 3). The ability of Ru to induce this I–M transition persists as the average size of the A site cations decreases, as shown for the $Nd_{0.4}Ca_{0.6}Mn_{1-x}Ru_xO_3$ series, whose $\rho(T)$ curve for $x = 0.06$ still exhibits an I–M transition at $T_C = 240$ K, the second maximum at 130 K being observed, whereas for $x = 0.10$ the double bump is obtained (Fig. 4). This behavior is corroborated by the magnetization measurements (inset of Fig. 4): the Nd

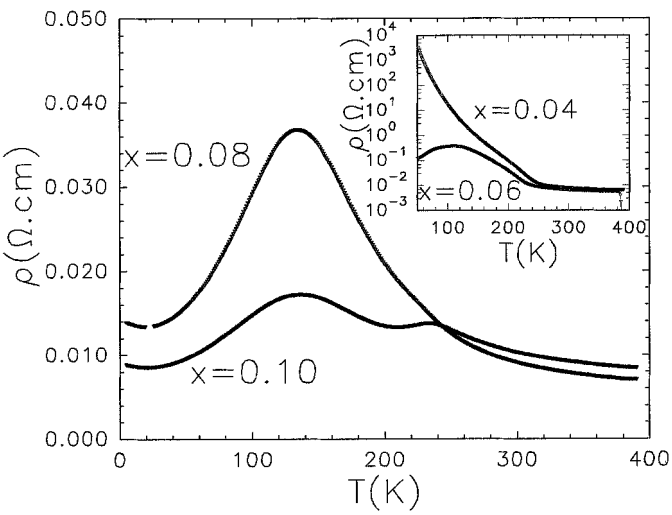

FIG. 5. $\rho(T)$ curves of $Sm_{0.4}Ca_{0.6}Mn_{1-x}Ru_xO_3$ ($x = 0.08$; $x = 0.10$). Inset: $x = 0.04$, $x = 0.06$.

$x = 0.06$ sample shows a high magnetic moment of 2.8 μ_B per Mn at 4 K as $Pr_{0.4}Ca_{0.6}Mn_{0.94}Ru_{0.06}O_3$, whereas for $x = 0.10$ the magnetic moment at 5 K decreases to 2.5 μ_B. Nevertheless, it should be emphasized that, as the average size of the A cation ($\langle r_A \rangle$) decreases, the effect of Ru upon the CO becomes less efficient, as shown from the $\rho(T)$ curves of the series $Sm_{0.4}Ca_{0.6}Mn_{1-x}Ru_xO_3$ (Fig. 5). For $x = 0.04$, the sample remains an insulator at low temperatures, in contrast to $Ln =$ La, and the I–M transition temperature decreases to 100 K for $x = 0.06$ (inset of Fig. 5) against 240 K for 6% Ru in $Pr_{0.4}Ca_{0.6}MnO_3$ (Fig. 3).

These results show that in a first step, ruthenium weakens the charge ordering in the Mn(IV)-rich manganites, but this effect is not sufficient to explain the appearance of ferromagnetism and metallicity at low temperature and especially the "double bump" phenomenon on the $\rho(T)$ curves. The present results can be explained on the basis of the phase separation scenario (11). For low Ru doping levels ($x \approx 0.02$ for Pr), FM clusters are formed around the Ru cations within the AFM "Mn^{3+}/Mn^{4+}" matrix (Fig. 6a); thus charge ordering coexists with these clusters and resistivity is not significantly affected. For higher doping levels ($x \approx 0.06$ for Pr) large metallic FM regions coexist with insulating AFM regions (Fig. 6b) so that the percolation threshold is reached. Electron diffraction study at low temperatures evidenced the presence of very weak, often scarcely visible, extra reflections. They are the signature of the presence of small CO domains and lend support to this hypothesis. In this case the FM regions are responsible for the observed high-temperature resistivity decrease at T_C on the $\rho(T)$ curves, which corresponds to the I–M transition within the FM regions. The second bump at lower temperatures corresponds then to the competitive contribution of both regions, AFM insulating and FM metallic, to the conductivity. While the details will be published separately, we note that the second ρ bump observed below T_C suggests that since the samples are not fully ferromagnetic, there remains

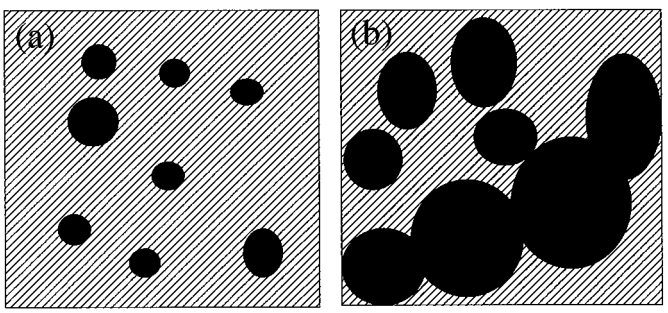

FIG. 6. Phase separation scenario in Ru-doped $Ln_{0.4}Ca_{0.6}Mn_{1-x}Ru_xO_3$ manganites: darkened regions correspond to ferromagnetism which develops around Ru ions in the AFM matrix (hatched region). (a) $x \approx 0.02$, FM clusters; (b) $x \approx 0.04$, the FM regions arrangement is close to the percolation threshold.

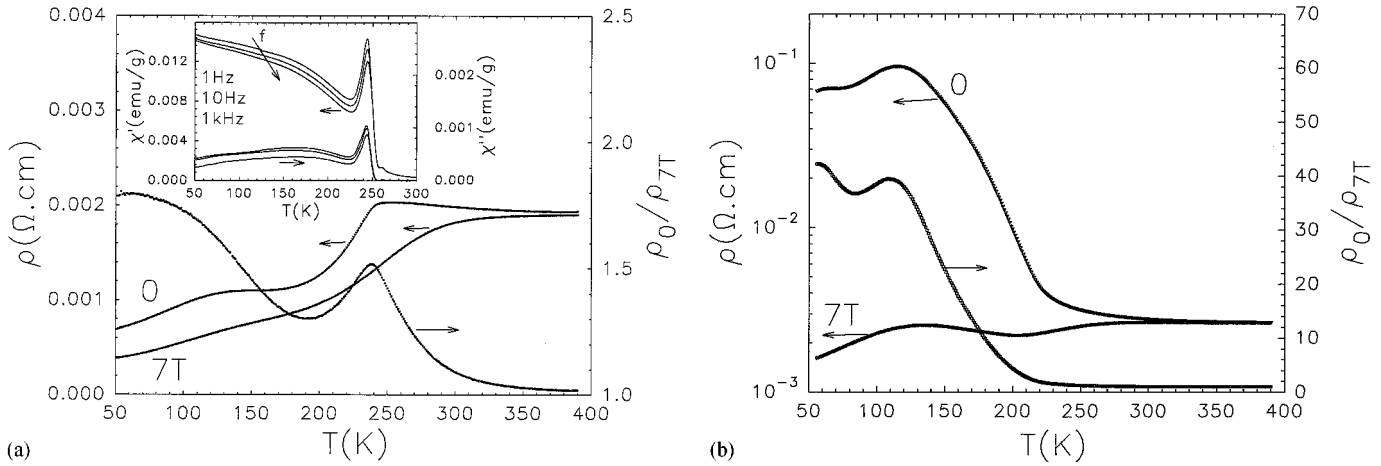

FIG. 7. $\rho(T)$ curves registered upon cooling in 0 and 7 T (left y-axis) and $\rho_0(T)/\rho_{7T}(T)$ ratio (right y-axis) for $Pr_{0.4}Ca_{0.6}Mn_{1-x}Ru_xO_3$ with $x = 0.06$ (a) and $x = 0.04$ (b). Inset of (a): T dependence of the ac susceptibility (χ', χ'' are the real and imaginary parts) of the corresponding $Pr_{0.4}Ca_{0.6}Mn_{0.94}Ru_{0.06}O_3$ sample.

a strong competition between AFM regions and FM regions in these Mn(IV)-rich samples. The cluster nature of our compounds is confirmed by the ac susceptibility curves (χ', χ'' vs T) of the $Pr_{0.4}Ca_{0.6}Mn_{0.94}Ru_{0.06}O_3$ sample (inset of Fig. 7a) which show strong frequency dependence over a wide temperature range below the onset of intracluster ferromagnetism at $T \approx 250$ K. We are looking into the finer details. The $\chi'(T)$ curve shows a main peak just below T_C ($T_C = 255$ K from the appearance of dissipation on the $\chi''(T)$ curve) and a broad shoulder below that peak where frequency effects are evidenced. Such $\chi'(T)$ and $\chi''(T)$ curves have already been observed in cluster-glass type cobaltites (12), which is in agreement with the cluster scenario proposed for these Ru-doped $Ln_{0.4}Ca_{0.6}MnO_3$ manganites.

The role of ruthenium in the appearance of FM clusters and their large domains (schematically drawn in Fig. 6b) can be explained by the ability of this element to exhibit two superior oxidation states, Ru(IV) and Ru(V), in oxides, and especially in perovskites when they are prepared in air or under oxygen. This is indeed the case for the perovskites A_2LnRuO_6 with A = Ca, Sr, Ba and Ln = Nd, Ho, Er, Lu, Y (13, 14), and $BaLaMRuO_6$ with M = Zn, Fe (15), which were shown to contain only Ru(V) when prepared in air, whereas Ru valence states ranging from 4.1 to 4.9 were observed for the perovskites $(Sr, La)_1(M, Ru)_1O_3$ with M = Li, Na, Mg (16). The great stability of Ru(V) in air is moreover not limited to perovskites, as shown for the 1D compound La_3RuO_7 (17). Thus, from these observations, the presence of Ru(V) and Ru(IV) species appears most probable and should be considered as an explanation for the appearance of ferromagnetism. The electronic configuration of Ru(V), t_{2g}^3, is similar to that of Mn(IV); Ru(IV), $t_{2g}^4e_g^0$, differs from Mn(III), $t_{2g}^3e_g^1$, with extra spin being at the t_{2g} level rather than at the e_g level. Mn(III) can interact with both Ru(IV) and Ru(V) via ferromagnetic superexchange interaction involving overlap of the less than half-filled e_g orbital of Mn(III) and the empty e_g orbitals of Ru(IV) and Ru(V) (14). Thus its introduction onto the Mn lattice not only tends to destroy the charge ordering but may contribute to the increase in Mn^{3+} content according to the equilibrium $Mn^{4+} + Ru^{4+} \leftrightharpoons Mn^{3+} + Ru^{5+}$. Consequently FM metallic clusters are generated not only by DE between Mn species ($Mn^{3+} + Mn^{4+} \leftrightharpoons Mn^{4+} + Mn^{3+}$), but also by the FM superexchange interactions (18) between Mn(III) and both Ru(IV) and Ru(V). Thus it is most probable that the FM clusters are formed around the Ru cations; the latter destroy charge ordering locally and simultaneously favor double exchange.

Finally it should be emphasized that the Ru-doped manganites exhibit magnetoresistance properties despite their metallic conductivity. This is illustrated by the $\rho(T)$ curve of the Pr-$x = 0.06$ sample registered under 7 T (Fig. 7a), which shows a maximum resistance ratio $RR = R_{0T}/R_{7T}$ of 1.5 at T_C, whereas the undoped phase does not show any MR. But, more important, CMR will be of course enhanced in a spectacular manner, for lower doping levels, when smaller FM domains coexist with AFM regions, as shown for the Pr-$x = 0.04$ sample (Fig. 7b), which exhibits a RR value of 40 at 110 K. The latter result shows that the AFM regions shrink under an external magnetic field, giving rise to enlargement of FM clusters and eventually leading to percolation.

In conclusion, ruthenium doping is shown to be an efficient method of inducing an I–M transition in Mn(IV)-rich manganites. This behavior can be explained in the framework of the phase separation scenario by the formation of

FM clusters around Ru, which grow rapidly with the Ru content, forming large regions in the AFM matrix. Moreover, the effect of ruthenium is different from that of chromium, since higher T_C's are reached for the former. This particular aptitude for inducing ferromagnetism and metallicity is above all supported by the possible existence of two oxidation states, Ru(IV) and Ru(V), which are isoelectronic to Mn(III) and Mn(IV), respectively, so that ferromagnetic coupling may exist between Mn and Ru, in contrast to the antiferromagnetic coupling which exists between Cr and Mn cations (19). Consequently, higher T_C's can be reached.

ACKNOWLEDGMENT

R. Mahendiran thanks the French Minister of Education and Research for supporting his stay with a fellowship.

REFERENCES

1. C. Zener, *Phys. Rev.* **82,** 403 (1951).
2. P. G. de Gennes, *Phys. Rev.* **118,** 141 (1960).
3. A. Maignan, F. Damay, A. Barnabé, C. Martin, M. Hervieu, and B. Raveau, *Philos. Trans. R. Soc. London A Ser.* **356,** 1635 (1998).
4. B. Raveau, A. Maignan, and C. Martin, *J. Solid State Chem.* **130,** 162 (1997).
5. A. Maignan, F. Damay, C. Martin, and B. Raveau, *Mater. Res. Bull.* **32,** 965 (1997).
6. A. Barnabé, A. Maignan, M. Hervieu, F. Damay, C. Martin, and B. Raveau, *Appl. Phys. Lett.* **71,** 3907 (1991).
7. T. Kimura, Y. Tomioka, R. Kumai, Y. Okimoto, and Y. Tokura, *Phys. Rev. Lett.* **83,** 3940 (1999).
8. R. Mahendiran, M. Hervieu, A. Maignan, C. Martin, and B. Raveau, submitted for publication.
9. A. Barnabé, A. Maignan, M. Hervieu, and B. Raveau, *Eur. Phys. J. B* **1,** 145 (1998).
10. P. V. Vanitha, A. Arulraj, A. R. Raju, and C. N. R. Rao, *C. R. Acad. Sci. Paris* **2**(11–13), 595 (1999).
11. A. Moreo, S. Yunoki, and E. Dagotto, *Science* **283,** 2034 (1999); M. Uehara, S. Mori, C. Chen, and S. W. Cheong, *Nature* (*London*) **399,** 560 (1999). See also R. Mahendiran, M. R. Ibarra, A. Maignan, C. Martin, B. Raveau, and A. Hernando, *Solid State Commun.* **111,** 525 (1999) and references therein.
12. S. Mukherjee, R. Ranganathan, P. S. Anilkumar, and P. A. Joy, *Phys. Rev. B* **54,** 9267 (1996).
13. P. D. Battle and C. W. Jones, *J. Solid State Chem.* **78,** 108 (1989).
14. P. D. Battle, C. W. Jones, and F. Studer, *J. Solid State Chem.* **90,** 302 (1991).
15. P. D. Battle, T. Gibb, C. W. Jones, and F. Studer, *J. Solid State Chem.* **78,** 281 (1989).
16. I. Kim, T. Nakamura, M. Itoh, and Y. Inaguma, *Mater. Res. Bull.* **28,** 1029 (1993).
17. P. Khalifah, R. W. Erwin, J. W. Lynn, Q. Wang, B. Battlog, and R. J. Cava, *Phys. Rev. B* **60,** 9573 (1999).
18. J. B. Goodenough, A. Woid, R. J. Arrot, and N. Menyuk, *Phys. Rev. B* **124,** 373 (1961).
19. F. Studer, O. Toulemonde, J. B. Goedkoop, A. Barnabé, and B. Raveau, *Jpn. J. Appl. Phys.* **38,** 377 (1999).